

Search for $K^+ \rightarrow \pi^+ \nu \bar{\nu}$ at CERN

Michele Corvino^{*†}

University and INFN Naples, Italy

E-mail: corvino@na.infn.it

The decay $K^+ \rightarrow \pi^+ \nu \bar{\nu}$, with a very precisely predicted branching ratio of less than 10^{-10} , is one of the best candidates to reveal indirect effects of new physics at the highest mass scales. The NA62 experiment at CERN SPS is designed to measure the branching ratio of the $K^+ \rightarrow \pi^+ \nu \bar{\nu}$ with a decay-in-flight technique, novel for this channel. NA62 took data in 2016, 2017 and 2018. Statistics collected in 2016 allows NA62 to reach the Standard Model sensitivity for $K^+ \rightarrow \pi^+ \nu \bar{\nu}$, entering the domain of 10^{-10} single event sensitivity and showing the proof of principle of the experiment. The data analysis is reviewed and the preliminary result from the 2016 data set presented.

*The 9th International workshop on Chiral Dynamics
17-21 September 2018
Durham, NC, USA*

^{*}Speaker.

[†]On behalf of the NA62 Collaboration: R. Aliberti, F. Ambrosino, R. Ammendola, B. Angelucci, A. Antonelli, G. Anzivino, R. Arcidiacono, M. Barbanera, A. Biagioni, L. Bician, C. Biino, A. Bizzeti, T. Blazek, B. Bloch-Devau, V. Bonaiuto, M. Boretto, M. Bragadireanu, D. Britton, F. Brizioli, M.B. Brunetti, D. Bryman, F. Bucci, T. Capussela, A. Ceccucci, P. Cenci, V. Cerny, C. Cerri, B. Checcucci, A. Conovaloff, P. Cooper, E. Cortina Gil, M. Corvino, F. Costantini, A. Cotta Ramusino, D. Coward, G. D'Agostini, J. Dainton, P. Dalpiaz, H. Danielsson, N. De Simone, D. Di Filippo, L. Di Lella, N. Doble, B. Dobrich, F. Duval, V. Duk, J. Engelfried, T. Enik, N. Estrada-Tristan, V. Falaleev, R. Fantechi, V. Fascianelli, L. Federici, S. Fedotov, A. Filippi, M. Fiorini, J. Fry, J. Fu, A. Fucci, L. Fulton, E. Gamberini, L. Gatignon, G. Georgiev, S. Ghinescu, A. Gianoli, M. Giorgi, S. Giudici, F. Gonnella, E. Goudzovski, C. Graham, R. Guida, E. Gushchin, F. Hahn, H. Heath, T. Husek, O. Hutanu, D. Hutchcroft, L. Iacobuzio, E. Iacopini, E. Imbergamo, B. Jennings, K. Kampf, V. Kekelidze, S. Kholodenko, G. Khorauli, A. Khotyantsev, A. Kleimenova, A. Korotkova, M. Koval, V. Kozhuharov, Z. Kucerova, Y. Kudenko, J. Kunze, V. Kurochka, V. Kurshetsov, G. Lanfranchi, G. Lamanna, G. Latino, P. Laycock, C. Lazzeroni, M. Lenti, G. Lehmann Miotto, E. Leonardi, P. Lichard, L. Litov, R. Lollini, D. Lomidze, A. Lonardo, P. Lubrano, M. Lupi, N. Lurkin, D. Madigozhin, I. Mannelli, G. Mannocchi, A. Mapelli, F. Marchetto, R. Marchevski, S. Martellotti, P. Massarotti, K. Massri, E. Maurice, M. Medvedeva, A. Mefodev, E. Menichetti, E. Migliore, E. Minucci, M. Mirra, M. Misheva, N. Molokanova, M. Moulson, S. Movchan, M. Napolitano, I. Neri, F. Newson, A. Norton, M. Noy, T. Numao, V. Obraztsov, A. Ostankov, S. Padolski, R. Page, V. Palladino, C. Parkinson, E. Pedreschi, M. Pepe, M. Perrin-Terrin, L. Peruzzo, P. Petrov, F. Petrucci, R. Piandani, M. Piccini, J. Pinzino, I. Polenkevich, L. Pontisso, Yu. Potrebenikov, D. Protopopescu, M. Raggi, A. Romano, P. Rubin, G. Ruggiero, V. Ryjov, A. Salamon, C. Santoni, G. Saracino, F. Sargeni, V. Semenov, A. Sergi, A. Shaikhiev, S. Shkarovskiy, D. Soldi, V. Sougonyaev, M. Sozzi, T. Spadaro, F. Spinella, A. Sturgess, J. Swallow, S. Trilov, P. Valente, B. Velghe, S. Venditti, P. Vicini, R. Volpe, M. Vormstein, H. Wahl, R. Wanke, B. Wrona, O. Yushchenko, M. Zamkovsky, A. Zinchenko.

1. The $K^+ \rightarrow \pi^+ \nu \bar{\nu}$ decay

The $K^+ \rightarrow \pi^+ \nu \bar{\nu}$ decay is a flavour-changing neutral current process, suppressed in the Standard Model (SM) by the GIM mechanism. The dominant contribution comes from short distance top quark loop, with negligible long distance physics dependence. Moreover, the hadron matrix element largely cancels when normalized to experimentally well known $K^+ \rightarrow \pi^0 e^+ \nu$ decay, making the theoretical prediction for the branching ratio very accurate: [1]

$$BR(K^+ \rightarrow \pi^+ \nu \bar{\nu}) = (8.4 \pm 0.1) \times 10^{-11} \quad (1.1)$$

The largest source of theoretical uncertainty comes from the knowledge of CKM matrix elements. The SM suppression and the theoretical accuracy makes this decay a golden candidate to search for new physics, in a complementary way with respect to the ones performed at colliders.

The most recent measurement of the BR has been obtained by the E949 collaboration at BNL in 2009 using kaons decaying at rest [2]:

$$BR(K^+ \rightarrow \pi^+ \nu \bar{\nu}) = (1.73^{+1.15}_{-1.05}) \times 10^{-10} \quad (1.2)$$

2. The NA62 experiment at CERN

NA62 is a fixed target experiment located in the CERN North Area in which kaons decay in flight. The schematic layout of the experiment is reported in Figure 1. A primary beam of 400 GeV/c protons coming from the CERN SPS is focused onto a beryllium target to produce a not-separated beam with a momentum of 75 GeV/c and a nominal rate of 800 MHz. The total length of NA62 apparatus, starting from the target, is ~ 270 m.

The secondary beam is mostly made by pions and protons, with only 6% of K^+ component. Kaons in the initial state are identified by the KTAG, a differential Cherenkov counter, and their momentum is measured by a three-station silicon tracker (GTK). To protect from events in which kaons interact with the last GTK station (GTK3), producing low angle pions that can mimic a signal, a veto detector (CHANTI) is used. The decay region starts after the CHANTI and is surrounded by the Large Angle Veto system (LAV), which is used to reject photons in the final state up to 50 mrad. Downstream tracks momenta are measured by a 4-chambers STRAW tracker and the particle identification is performed by a RICH detector. A charged hodoscopes system (CHOD) is used to provide a time input for the trigger with 200 ps time resolution. The photon veto system hermeticity at low angles is ensured by a liquid krypton electromagnetic calorimeter (LKr) and two small angle calorimeters (IRC and SAC). Muons are rejected by a three-stations veto system, located downstream the LKCr. The first two stations are used as hadronic calorimeter while the third one (MUV3) is placed downstream a 80 cm thick iron wall. Additional vetoes (MUV0, HASC) provide further background rejection power. A more detailed description of the apparatus can be found in [3].

A multilevel trigger is used to collect data with different trigger streams; the $K^+ \rightarrow \pi \nu \bar{\nu}$ events are collected with a dedicated trigger stream which uses RICH, CHOD to select a single track and LKCr, LAV and MUV3 as veto. A minim bias trigger stream is also used for normalization and background evaluation. The two trigger streams are referred as "PNN" and "control" respectively.

The experiment has taken data from 2016 to 2018. In the following, the analysis of 2016 dataset, corresponding to 2% of the total sample, is reported.

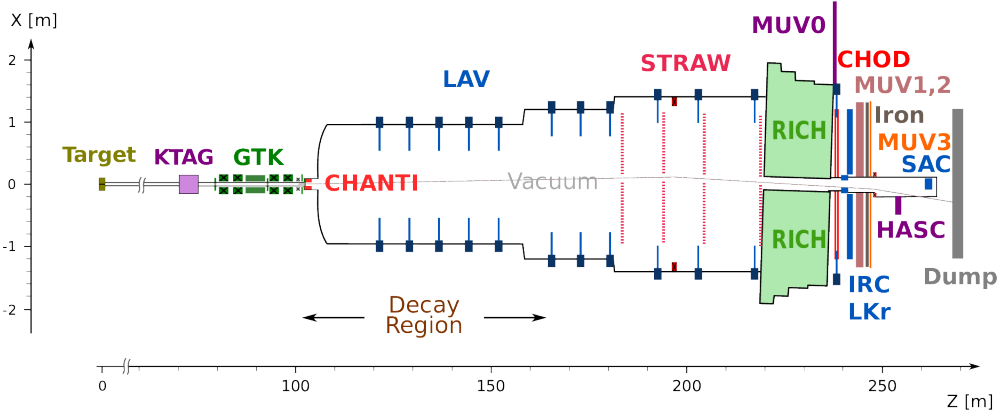


Figure 1: Schematics of NA62 apparatus

3. Event selection

The experimental signature of $K^+ \rightarrow \pi^+ \nu \bar{\nu}$ is extremely poor: only a charged particle, identified as a pion, in time with the upstream kaon while the neutrinos are not detected. The signal selection proceeds through the following steps: the events must have single track reconstructed in the downstream detectors; the track must be identified as a pion and it has to be associated to an upstream K; no activity in time has to be present in the photon and muon veto systems; a kinematic selection is applied to define signal and background regions.

A blind analysis technique is adopted so that events in signal regions have been looked at only after the complete background evaluation. Signal events have been considered in the pion momentum range [15-35] GeV/c, in order to improve the background rejection having at least 40 GeV/c of missing energy. Main background sources are $K^+ \rightarrow \mu^+ \nu_\mu$ (namely $K_{\mu 2}$), $K^+ \rightarrow \pi^+ \pi^0$ ($K_{2\pi}$) and $K^+ \rightarrow \pi^+ \pi^+ \pi^-$ ($K_{3\pi}$) events which enter the signal regions because of resolution effects, radiative decays of the former two, $K^+ \rightarrow l^+ \pi^0 \nu$ ($l = \mu, e$) or more rare processes like $K^+ \rightarrow \pi^+ \pi^- e^+ \nu$ not constrained in the m_{miss}^2 distribution by the neutrinos in the final state. Other backgrounds to be taken into account are due to K^+ decays in the region upstream the GTK and the events in which an inelastic interaction between the beam and GTK3 occurs.

The kinematic selection is based on the measurement of the variable $m_{miss}^2 = (P_K - P_\pi)^\mu (P_K - P_\pi)_\mu$, whose distribution is reported in Figure 2. Two signal regions are defined: region 1 (R1), between $K_{\mu 2}$ and $K_{2\pi}$ peaks, and region 2 (R2), between the distributions of $K_{2\pi}$ and $K_{3\pi}$. The m_{miss}^2 resolution is $\sigma(m_{miss}^2) = 1 \times 10^{-3} \text{ GeV}^2/c^4$. To protect against kinematic mis-reconstruction, additional constraints are imposed on the m_{miss}^2 ($RICH, GTK$) and m_{miss}^2 ($STRAW, Beam$) variables, computed by replacing in the m_{miss}^2 definition the momentum from STRAW with the one measured by the RICH under a π^+ mass hypothesis and the GTK momentum with the nominal beam value respectively.

Pion identification is performed combining informations from RICH and calorimeters: the particle-ID efficiency is 64% with a μ^+ mis-identification probability of 10^{-8} . Events with π^0 in

the final state are rejected looking at the in-time activity in LAV, LKr, IRC and SAC; the rejection factor is 3×10^{-8} , measured counting the number of $K_{2\pi}$ events collected with control and PNN and trigger streams, before and after the photon rejection criteria respectively.

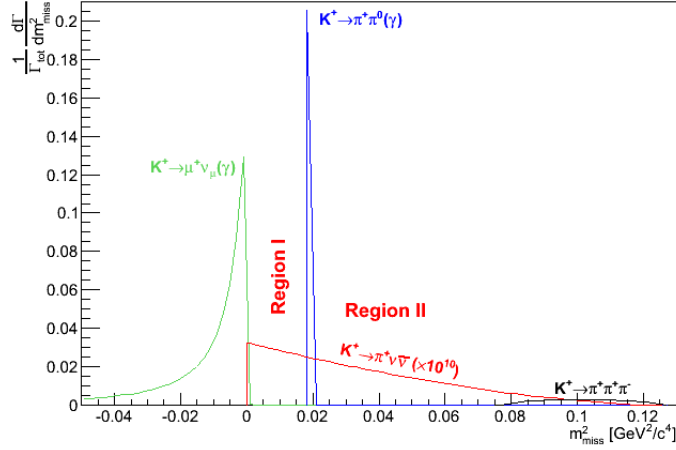


Figure 2: m_{miss}^2 distribution for the signal and the main background channels. Note that the signal distribution has been multiplied by a factor 10^{10} .

4. Expected signal and background events

4.1 Single Event Sensitivity (SES)

The SES is defined as following:

$$SES = \frac{1}{N_K \cdot \varepsilon_{\pi\nu\nu}} \quad (4.1)$$

where N_K is the number of kaon decays in the decay region and $\varepsilon_{\pi\nu\nu}$ is the signal efficiency. The former has been computed using $K_{2\pi}$ decay as normalization channel: $N_K = (N_{K_{2\pi}} \cdot D) / (A_{K_{2\pi}} \cdot BR(K_{2\pi}))$. $N_{K_{2\pi}}$ is counted using control-triggered events and the factor $D = 400$ corresponds to the downscale factor between the two trigger streams. The number of collected kaon decays is $N_K = (1.21 \pm 0.02) \times 10^{11}$.

The selection efficiency has been evaluated in 4 bins of downstream track momentum, from 15 to 35 GeV/c. In each of those bins, the efficiency is given by the product of three different factors:

$$\varepsilon_{\pi\nu\nu} = \sum_i Acc_{\pi\nu\nu}^i \cdot \varepsilon_{trigg}^i \cdot \varepsilon_{RV}^i \quad (4.2)$$

$Acc_{\pi\nu\nu}$ is the signal acceptance, which is 4%, divided between R1(1%) and R2(3%); ε_{trigg} is the PNN trigger efficiency and ε_{RV} is a factor that correspond to the fraction of events which are not vetoed because of random activity in the veto system. This factor ("random veto") has been measured selecting a sample of $K_{\mu 2}$ and applying to it the full photon and multiplicity rejection criteria. The SES and the number of expected signal events are:

$$SES = (3.15 \pm 0.01_{stat} \pm 0.24_{syst}) \times 10^{-10} \quad (4.3)$$

Process	Expected events
$K^+ \rightarrow \pi \nu \bar{\nu} (SM)$	$0.267 \pm 0.001_{stat} \pm 0.020_{syst} \pm 0.032_{ext}$
$K^+ \rightarrow \pi^+ \pi^0 (\gamma)$	$0.064 \pm 0.007_{stat} \pm 0.006_{syst}$
$K^+ \rightarrow \mu^+ \nu (\gamma)$	$0.02 \pm 0.003_{stat} \pm 0.006_{syst}$
$K^+ \rightarrow \pi^+ \pi^- e^+ \nu$	$0.018^{+0.024}_{-0.017} _{stat} \pm 0.009_{syst}$
$K^+ \rightarrow \pi^+ \pi^+ \pi^-$	$0.002 \pm 0.001_{stat} \pm 0.002_{syst}$
Upstream background	$0.050^{+0.090}_{-0.030} _{stat}$
Total background	$0.15 \pm 0.09_{stat} \pm 0.01_{syst}$

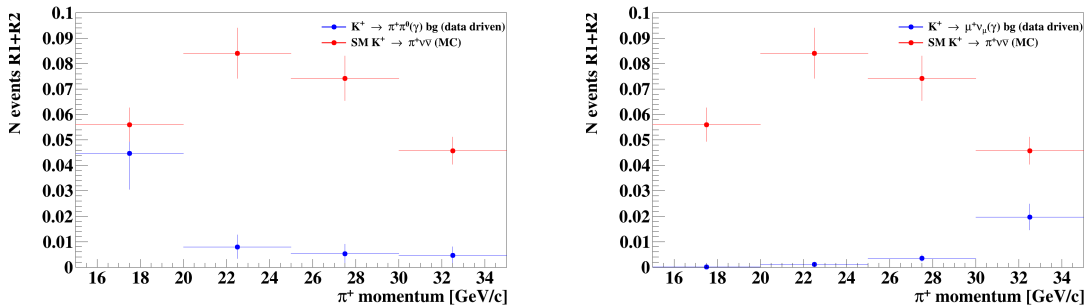
Table 1: Expected signal and background events

$$N_{\pi\nu\nu}^{exp}(SM) = 0.267 \pm 0.001_{stat} \pm 0.020_{syst} \pm 0.032_{ext} \quad (4.4)$$

The systematic uncertainty on SES is mostly due to the error on random veto (0.17×10^{-10}), with other contribution coming from the definition of normalization region (0.10×10^{-10}) and from the estimation of signal acceptance (0.09×10^{-10}).

4.2 Background evaluation

$K^+ \rightarrow \pi^+ \pi^0 (\gamma)$, $K^+ \rightarrow \mu^+ \nu_\mu (\gamma)$ and $K^+ \rightarrow \pi^+ \pi^+ \pi^-$ events may enter in the signal regions because of m_{miss}^2 mis-reconstruction; the expected background events for these decay modes are evaluated on data as the number of events in the background regions after the full PNN selection multiplied by the fraction of the m_{miss}^2 distributions entering the signal regions ("kinematic tails"). In Figure 3 the number of expected $K^+ \rightarrow \pi^+ \pi^0 (\gamma)$ and $K^+ \rightarrow \mu^+ \nu_\mu (\gamma)$ events in bins of P_π^+ are shown. Another relevant source of background is represented by $K^+ \rightarrow \pi^+ \pi^- e^+ \nu_e$ and have been

**Figure 3:** Distributions of expected $K_{2\pi}$ (left) and $K_{\mu 2}$ (right) background events in bins of downstream track momentum. The expected number of signal events in each bin is shown for comparison.

evaluated using 400 millions MonteCarlo events; the simulation has been validated using data in 5 independent regions. The uncertainty on the expected K_{e4} events is essentially due to the limited MC sample available. Finally, the upstream background has been evaluated using a data driven method. A summary on the expected signal and background events is reported in Table 1.

5. Results and conclusions

After the unblinding of the signal regions, one event has been found. The unblinded signal regions and the RICH ring for the signal event are shown in Figure 4. The corresponding upper limit, given by CLs method [4], is:

$$BR(K^+ \rightarrow \pi^+ \nu \bar{\nu}) < 14 \times 10^{-10} \quad @95\%CL \quad (5.1)$$

This result, based on 2% of the total 2016-2018 dataset, has to be intended as a proof of principle of the decay in flight technique, demonstrating the validity of NA62 approach. The measurement using the full data sample is in progress, analysis improvements are foreseen to reduce the background and enhance the signal efficiency.

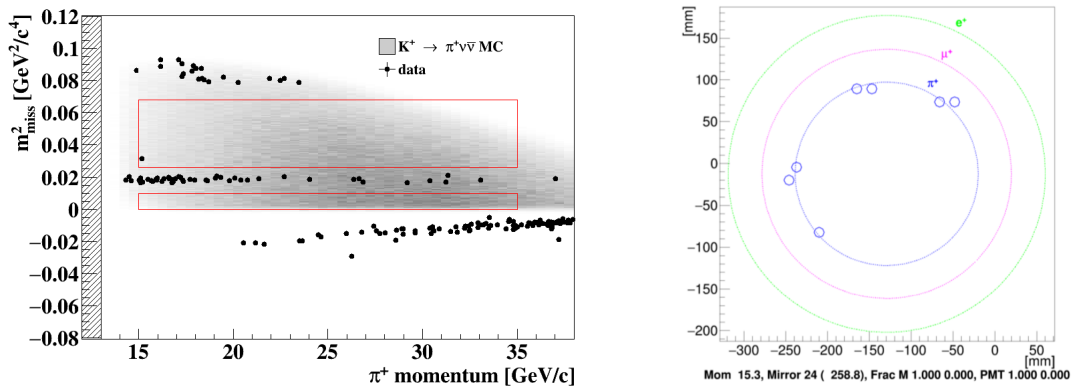


Figure 4: Left: m^2_{miss} distribution as a function of downstream track momentum after the unblinding of the signal regions, shown in red. Right: RICH response for the event found in R2, with superimposed rings in π , μ and e masses hypotheses.

References

- [1] Buras, A.J., Buttazzo, D., Girschbach-Noe, J. et al. J. High Energ. Phys. (2015) 2015: 33. [https://doi.org/10.1007/JHEP11\(2015\)033](https://doi.org/10.1007/JHEP11(2015)033)
- [2] A. V. Artamonov et al. (BNL-E949 Collaboration), Phys. Rev.D79(2009) 092004
- [3] E. Cortina Gil et al 2017, JINST 12 P05025
- [4] A. L. Read, J. Phys.G28(2002) 2693